Circulation
Cardiovascular Genetics

Transforming Growth Factor-β and Inflammation in Vascular (Type IV) Ehlers –Danlos Syndrome

Rachel Morissette, Florian Schoenhoff, Zhi Xu, David A. Shilane, Benjamin F. Griswold, Wuyan Chen, Jiandong Yang, Jie Zhu, Justyna Fert-Bober, Leslie Sloper, Jason Lehman, Natalie Commins, Jennifer E. Van Eyk and Nazli B. McDonnell

Circ Cardiovasc Genet. 2014;7:80-88; originally published online January 6, 2014;
doi: 10.1161/CIRCGENETICS.113.000280
Circulation: Cardiovascular Genetics is published by the American Heart Association, 7272 Greenville Avenue, Dallas, TX 75231

Print ISSN: 1942-325X. Online ISSN: 1942-3268

Transforming Growth Factor-β and Inflammation in Vascular (Type IV) Ehlers–Danlos Syndrome

Rachel Morissette, PhD; Florian Schoenhoff, MD; Zhi Xu, PhD; David A. Shilane, PhD; Benjamin F. Griswold, BS; Wuyan Chen, PhD; Jiandong Yang, PhD; Jie Zhu, MS; Justyna Fert-Bober, PhD; Leslie Sloper, RN; Jason Lehman, MD; Natalie Commins, BA; Jennifer E. Van Eyk, PhD; Nazli B. McDonnell, MD, PhD

Background—Vascular Ehlers–Danlos syndrome (VEDS) causes reduced life expectancy because of arterial dissections/rupture and hollow organ rupture. Although the causative gene, *COL3A1*, was identified >20 years ago, there has been limited progress in understanding the disease mechanisms or identifying treatments.

Methods and Results—We studied inflammatory and transforming growth factor-β (TGF-β) signaling biomarkers in plasma and from dermal fibroblasts from patients with VEDS. Analyses were done in terms of clinical disease severity, genotype–phenotype correlations, and body composition and fat deposition alterations. VEDS subjects had increased circulating TGF-β1, TGF-β2, monocyte chemotactic protein-1, C-reactive protein, intercellular adhesion molecule-1, vascular cell adhesion molecule-1, and leptin and decreased interleukin-8 versus controls. VEDS dermal fibroblasts secreted more TGF-β2, whereas downstream canonical/noncanonical TGF-β signaling was not different. Patients with *COL3A1* exon skipping mutations had higher plasma intercellular adhesion molecule-1 and vascular cell adhesion molecule-1, and VEDS probands had abnormally high plasma C-reactive protein versus affected patients identified through family members before any disease manifestations. Patients with VEDS had higher mean platelet volumes, suggesting increased platelet turnover because of ongoing vascular damage, as well as increased regional truncal adiposity.

Conclusions—These findings suggest that VEDS is a systemic disease with a major inflammatory component. C-reactive protein is linked to disease state and may be a disease activity marker. No changes in downstream TGF-β signaling and increased platelet turnover suggest that chronic vascular damage may partially explain increased plasma TGF-β1. Finally, we found a novel role for dysregulated TGF-β2, as well as adipocyte dysfunction, as demonstrated through reduced interleukin-8 and elevated leptin in VEDS. **(*Circ Cardiovasc Genet*. 2014;7:80-88.)**

Key Words: aneurysm ■ biomarkers ■ Ehlers-Danlos syndrome ■ extracellular matrix ■ inflammation

Vascular Ehlers–Danlos syndrome (VEDS), formerly known as type IV EDS, leads to reduced life expectancy because of arterial dissections and rupture, as well as hollow organ rupture, with life-threatening complications occurring as early as the second decade of life.[1] Despite the identification of the causative gene, *COL3A1*, >2 decades ago,[2–4] there has been limited progress on understanding the disease mechanism beyond that of connective tissue weakness because of structural defects or reduced amounts of type III procollagen. The only human treatment intervention trial to date was modestly beneficial to arterial complications using celiprolol, a mixed β(1)-adrenoceptor antagonist and β(2)-adrenoceptor agonist that is not available in the United States.[5] Although the drug mechanism remains unclear, a protective role for transforming growth factor-β (TGF-β) has been suggested.[5] In a *COL3A1* haploinsufficiency mouse model study, doxycycline, a matrix metalloproteinase inhibitor, reduced arterial lesions.[6] Whether this will be applicable to other mutations that disrupt the collagen triple helix is not known nor have the results been validated in humans.

Editorial see p 5
Clinical Perspective on p 88

The *COL3A1* gene product, procollagen III, is processed to form the mature collagen III homotrimer. The most common *COL3A1* mutations in VEDS are missense resulting in the substitution of other amino acids for glycine located throughout the triple-helical domain, with the next most common being splice site mutations that lead to single exon skipping (ES).[1,7] These mutation classes result in a dilated endoplasmic reticulum in skin fibroblasts, reduced type III procollagen secretion, elastic fiber abnormalities, and alterations in the size and distribution of the major collagen fibrils

Received May 28, 2013; accepted December 19, 2013.

From the Laboratory of Clinical Investigation, National Institute on Aging, Baltimore, MD (R.M., Z.X., B.F.G., W.C., J.Y., L.S., J.L., N.C., N.B.M.); Department of Medicine, Johns Hopkins Bayview Proteomics Center, Johns Hopkins University, Baltimore, MD (F.S., J.Z., J.F.-B., J.E.V.E.); Department of Cardiovascular Surgery, University Hospital Berne, Berne, Switzerland (F.S.); and Stanford University School of Medicine, Stanford, CA (D.A.S.).

The Data Supplement is available at http://circgenetics.ahajournals.org/lookup/suppl/doi:10.1161/CIRCGENETICS.113.000280/-/DC1.

Correspondence to Nazli McDonnell, MD, PhD, National Institute on Aging, National Institutes of Health, NIA Clinical Unit, 5th Floor, 3001 S. Hanover St, Baltimore, MD 21225. E-mail nazli.mcdonnell@gmail.com

through a dominant negative mechanism.[8] By contrast, haploinsufficiency null mutations that act via a protein deficiency mechanism result in a milder clinical phenotype with delayed vascular complication onset and absence of hollow organ rupture.[9,10] Comparing these patient groups based on mutation type and disease severity by disease-related biomarkers can help to delineate the disease process resulting from abnormally structured type III collagen.

With the emerging role of the TGF-β pathway in genetically mediated aneurysm syndromes such as Marfan syndrome (MFS)[11–13] and the identification of multiple TGF-β–related genes that cause syndromes phenotypically overlapping with VEDS,[14–16] we sought to study the role of this pathway in VEDS pathogenesis using patient-derived fibroblast cell lines and plasma. The 3 mammalian TGF-β isoforms, TGF-β1, TGF-β2, and TGF-β3, are known to regulate diverse biological processes and maintain tissue homeostasis; their functions are dependent on the relative expression of the isoforms in vivo.[17] In light of the catastrophic disease progression seen in some patients,[18] we quantified circulating biomarkers involved in vascular inflammation (TGF-β1, TGF-β2, monocyte chemotactic protein-1 [MCP-1], C-reactive protein [CRP], intercellular adhesion molecule-1 [ICAM-1], vascular cell adhesion molecule-1 [VCAM-1]) and their role in the natural history of VEDS. Because access to vascular tissue through clinical care is limited, dermal fibroblasts have been used to study features of genetic disorders,[19–21] which we used to study TGF-β biomarkers. The pleiotropic phenotypes seen in the VEDS setting, such as alterations in body composition and fat deposition and related biomarker expression (interleukin-8 [IL-8], leptin, adiponectin), clinical disease severity, and genotype–phenotype analyses, were correlated to biomarker concentrations to identify disease markers and treatment targets. In addition to evidence of systemic inflammation, we found a novel role for dysregulated TGF-β2 and adipocyte dysfunction as demonstrated through reduced IL-8 and elevated leptin in VEDS.

Methods

Study Subjects

All study patients were enrolled in protocol no. 2003–086, approved by the MedStar Health and the National Institute on Aging Institutional Review Board, and provided informed consent. Age- and sex-matched healthy controls were obtained from the Baltimore Longitudinal Study of Aging. Dual-energy x-ray absorptiometry studies on patients and Baltimore Longitudinal Study of Aging controls were performed on a GE Lunar Prodigy Advance scanner. Control plasma and skin biopsy samples were obtained with informed consent at the National Institute on Aging (no. 2003–086 and 2003–071). Additional deidentified human dermal fibroblasts from apparently healthy subjects with normal chromosomes and low passage were obtained from the Coriell repository (http://ccr.coriell.org). All disease complications occurred at least a year before sample collection, and patients were not acutely ill.

Genetic Mutation Analysis

All VEDS subjects included in this study have a pathogenic mutation confirmed in *COL3A1*. Details are available in the Data Supplement.

Fibroblast Cell Culture and ELISA Assays

Dermal fibroblasts were cultured from a 4-mm punch skin biopsy. Culture conditions, immunoblot methods, and biomarker ELISA methods are available in the Data Supplement.

COL3A1 Gene Silencing by Allele-Specific Small Interfering RNA (siRNA)

COL3A1 allele-specific gene silencing and protein knockdown in a VEDS patient fibroblast cell line with a glycine mutation [c.755G>T (G252V)] was performed as previously described.[22] Details are available in the Data Supplement. Experiments were done in triplicate.

Mean Platelet Volume and Clinical CRP Measurements

Clinical testing for mean platelet volume (MPV) and platelets (n=35 VEDS, 74 controls) was done using a Clinical Laboratory Improvement Amendments-certified, automatic blood counter (Sysmex XE-5000 Analyzer, Sysmex America, Inc, Lincolnshire, IL), and clinical CRP was measured from serum separator tubes using a Dimension Vista 3000T analyzer (Siemens, Erlangen, Germany) in the Harbor Hospital Clinical Laboratory, Baltimore, MD.

Statistical Analysis

Comparisons were made with the unpaired Student *t* test to assess mean differences. All *P* values are 2-tailed and considered significant when ≤0.05. Data are represented as mean±SEM. Because of the potential for correlations induced by related subjects, we also considered generalized estimating equations with an exchangeable correlation structure as an alternative method of comparison in assays that used related subjects. The normality of the data was checked by constructing quantile–quantile plots of each sample and biomarker. All statistical analyses were done using Microsoft Excel 2010 and R 2.10.1.

Results

VEDS Clinical Features

In our clinical cohort of 41 VEDS subjects, 30 were women (73.2%) and 11 were men (26.8%). Cardiovascular medications taken at the time of biological sample collection are listed in the Table. All patients were normotensive at the time of sample collection. Institutional review board approval did not allow for cardiovascular medication removal before the study visit.

Patients who have an arterial or a bowel event leading to a VEDS diagnosis are indicated in the Table. Two patients (patients 8 and 34) with ES mutations were identified as VEDS through severe bruising before experiencing an arterial or a bowel rupture. Thirteen patients were identified as VEDS through family members before any manifestations themselves, which we termed *I*dentified *T*hrough *F*amily *H*istory (ITFH); familial relationships in the cohort are indicated (Table).

Genetic Analysis

Pathogenic mutations in *COL3A1* included 19 patients with a glycine substitution in the collagen triple helix (gly),[26] 10 patients with a splice site mutation resulting in ES,[27] 8 patients with a null mutation resulting in haploinsufficiency (null),[10] 2 patients with a small insertion/deletion (indel), 1 patient with a large deletion (del), and 1 patient with a missense mutation resulting in a Pro-Ser change (Table). Mutations were submitted to the Ehlers–Danlos Syndrome Variant Database (http://eds.gene.le.ac.uk).

The missense mutation resulting in a proline to serine substitution in *COL3A1* was not reported as a single-nucleotide polymorphism in the 1000 genomes (http://www.1000genomes.org) or in >6500 exomes on the Exome Variant Server (http://evs.gs.washington.edu/EVS). In silico analysis (PROVEAN, http://provean.jcvi.org; SIFT, http://sift.jcvi.org; PolyPhen-2, http://genetics.bwh.harvard.edu/pph2) identified this mutation

Table. Demographics, Medical History, Symptoms, Physical Examination, and Genetic Features

Patient No.	Sex	Diagnosis Age, y	Sample Collection Age, y	Familial Relation	Mutation in *COL3A1**	Consequence of Mutation	Arterial Event	Bowel Event	Medications	Refs.
Patient 1	M	51	51	Proband	c.3070C>T, p.R1024X	Null	+	–	BB, ST, CCB	9
Patient 2	M	24	25	ITFH, son of patient 1	c.3070C>T, p.R1024X	Null	–	–	None	
Patient 3	F	50	51	ITFH, sister of patient 1	c.3070C>T, p.R1024X	Null	–	–	ST, ACE1	
Patient 4	F	54	55	ITFH, sister of patient 1	c.3070C>T, p.R1024X	Null	–	–	BB, ST, ASA, CCB	
Patient 5	M	26	27	ITFH, nephew of patient 1	c.3070C>T, p.R1024X	Null	–	–	None	
Patient 6	F	37	56	Proband	c.2356G>A, p.G786R	Gly	+	–	BB	
Patient 7	M	25	30	ITFH, son of patient 6	c.2356G>A, p.G786R	Gly	–	–	BB	23
Patient 8	F	11	12	Proband	c.997-2 A>G	ES	–	–	None	
Patient 9	M	40	41	ITFH, father of patient 8	c.997-2 A>G	ES	–	–	BB	
Patient 10	F	42	42	ITFH, aunt of patient 8	c.997-2 A>G	ES	+	–	None	
Patient 11	F	48	51	Proband	c.1501G>A, p.G501R	Gly	+	+	BB, ACE1, CCB	1
Patient 12	F	32	38	ITFH, niece of patient 11	c.1501G>A, p.G501R	Gly	–	–	None	1
Patient 13	M	27	46	Proband	c.636+5G>A	ES	+	–	ST, ACE1	7
Patient 14	F	28	47	ITFH, sister of patient 13	c.636+5G>A	ES	–	–	BB	
Patient 15	F	41	45	Proband	c.766delA, p.I256Yfx7	Null	+	–	None	
Patient 16	F	45	47	ITFH, sister of patient 15	c.766delA, p.I256Yfx7	Null	–	–	None	
Patient 17	M	51	52	Proband	c.548G>C, p.G183A	Gly	+	–	ST, ARB	
Patient 18	F	21	23	Proband, daughter of patient 17	c.548G>C, p.G183A	Gly	+	–	BB	
Patient 19†	F	17	36	ITFH	c.3499G>T, p.G1167C	Gly	–	–	None	
Patient 20†	F	12	14	ITFH, daughter of patient 19	c.3499G>T, p.G1167C	Gly	+	–	None	
Patient 21	F	37	38	Proband	c.2221G>A, p.G741S	Gly	+	–	None	
Patient 22	F	17	36	Proband	c.2816G>A,p.G939D	Gly	+	+	BB	24
Patient 23	F	52	56	Proband	c.665G>T, p.G222V	Gly	+	+	None	
Patient 24	F	36	47	Proband	c.1033G>A, p.G345R	Gly	+	–	BB, ST, ASA, ARB	1
Patient 25	M	23	26	Proband	c.755G>T, p.G252V	Gly	+	–	BB	
Patient 26	F	53	56	Proband	c.2284 G>C, p.G762R	Gly	+	–	None	
Patient 27	F	10	14	Proband	c.3563G>A, p.G1188E	Gly	–	–	None	
Patient 28	F	27	30	Proband	c.2285G>A, p.G762D	Gly	–	–	BB	
Patient 29	F	26	30	Proband	c.3545G>A, p.G1182E	Gly	+	+	ASA	
Patient 30	F	28	29	Proband	c.2123G>A, p.G708D	Gly	+	–	ARB	
Patient 31†	F	38	41	ITFH	c.1618G>A, p.G540R	Gly	–	–	None	
Patient 32	F	32	42	Proband	c.1347+1G>C	ES	+	+	BB, ST	25
Patient 33	F	9	12	Proband	c.1149+2T>C	ES	–	–	None	
Patient 34	M	22	25	Proband	c.2553+1delG	ES	–	–	None	
Patient 35	F	13	29	Proband	c.3039+1G>A	ES	+	+	BB	
Patient 36	F	23	28	Proband	c.3093+2T>C	ES	+	–	None	
Patient 37	M	39	43	Proband	c.2824-1G>A	Null	+	–	BB	9
Patient 38	F	32	33	Proband	c.1763_1769delGTGCTCCinsTAAG, p.G588_P590delinsVS	Small indel	+	+	ASA	
Patient 39	F	49	54	Proband	c.1106_1108delGAG, p.G369del	Small indel	+	–	BB, ASA, ARB	
Patient 40	F	38	43	Proband	c.1764_1871del	Large del	+	–	None	
Patient 41	F	39	41	Proband	c.4318C>T, p.P1440S	Missense	+	–	ASA	

ACE1 indicates angiotensin-converting enzyme inhibitor; ARB, angiotensin receptor blocker; ASA, aspirin; BB, β-blocker; CCB, calcium channel blocker; del, deletion; ES, splice site mutation resulting in skipping of the exon; F, female; Gly, glycine substitution in the collagen triple helix; indel, insertion/deletion; ITFH, identified through family history; M, male; null, null mutation resulting in haploinsufficiency; and ST, statin.

*Nomenclature is based on the coding sequence of the *COL3A1* gene (ENSG00000168542) with the adenosine of the annotated translation start codon defined as nucleotide position +1.

†Proband not part of the study.

as pathogenic. Several of these mutations have been previously identified in other studies as indicated in the Table.

Circulating TGF-β Cytokines and Secretion From Dermal Fibroblasts

We analyzed plasma samples from 35 VEDS subjects and 74 age-, sex-, and body mass index–matched controls matching ≥1:2. Circulating TGF-β1 was significantly higher in VEDS subjects versus controls (8.3±1.1 versus 2.5±0.4 ng/mL; $P<0.0001$). Similarly, VEDS subjects had significantly increased circulating total TGF-β2 in plasma (152.2±6.3 versus 101.3±2.0 pg/mL; $P<0.0001$; Figure 1A). TGF-β3 was measured, but all samples were below the lower detection limit.

Total TGF-β1 and TGF-β2 secretion from isolated human skin fibroblasts was measured in a subset of 33 subjects who provided biopsy samples and whose cell lines provided adequate in vitro cell growth, including 17 VEDS subjects (12 F/5 M, representing 7 gly, 3 ES, 3 null, and 4 other mutations) and 17 controls, who were chosen at random from the initial 74 by a blinded technician. TGF-β1 and -β3 secretion was not significantly different between groups (data not shown). However, secreted TGF-β2 was significantly elevated (47.9±0.7 versus 42.9±0.8 pg/mL per milligram protein; $P<0.0001$) in VEDS subjects versus controls (Figure 1B). Although the secretion difference was only ≈15%, the results were highly significant and recapitulated those from plasma. Plasma and in vitro secreted TGF-β2 levels were positively correlated ($r=0.53$).

Downstream TGF-β Biomarkers in Dermal Fibroblasts

Downstream canonical TGF-β biomarkers treated with TGF-β1 (pSmad2, pSmad1/5/8) and untreated noncanonical (extracellular signal-regulated kinase1/2, p-p38 mitogen-activated protein kinase) markers were analyzed by Western blot in the same subset of dermal fibroblasts as above (n=17 VEDS, 17 controls). No significant differences ($P>0.05$) were found in these proteins between patients with VEDS and controls (Figure 2A and 2B) when normalized to either loading controls or total protein for phosphorylated markers. In addition, there were no quantitative differences between the TGF-β receptor I and II in untreated VEDS and control fibroblasts (data not shown). The same results seen with TGF-β1 stimulation were found with TGF-β2 stimulation (data not shown). To investigate possible biomarkers further, a human TGF-β/bone morphogenetic protein signaling pathway mRNA array was used to screen genes of interest; quantitative polymerase chain reaction was used to validate any potential gene hits. On validation, no pathway genes were found to differ between patients with VEDS and healthy controls (see Data Supplement).

COL3A1 Allele-Specific siRNA Treatment

To further confirm that a dominant negative *COL3A1* mutation in VEDS was not affecting downstream TGF-β signaling, we used allele-specific siRNA knockdown in fibroblasts from a VEDs patient with a c.755G>T (G252V) mutation in *COL3A1* as previously described.[22] This knockdown essentially converted a Gly-type *COL3A1* mutation to a haploinsufficient mutation, allowing us to study the presence of abnormally structured collagen fibrils versus qualitative deficiency of type III collagen influence on TGF-β downstream signaling. Figure 3A shows that *COL3A1* mRNA and protein were knocked down compared with randomized siRNA. The TGF-β biomarkers were again tested by Western blot and showed no differences between the VEDS sample with the mutant allele knocked down and the same sample with the Gly mutation intact (Figure 3B).

Inflammatory Biomarkers and Adipokines in EDTA Plasma

VEDS plasma concentrations of MCP-1, CRP, ICAM-1, and VCAM-1 as well as leptin were all significantly elevated, whereas IL-8 was significantly decreased versus age- and sex-matched controls ($P=0.001$, $P=0.046$, $P=0.0004$, $P=0.0006$, $P=0.006$, $P<0.0001$, respectively; Figure 4A–4F). Plasma CRP concentrations were confirmed using a clinical immunoassay, and they were highly and positively correlated with the multiplex CRP assay ($r=0.93$). TNF-α, serum amyloid A, and adiponectin were not significantly different between groups according to a Meso Scale Discovery multiplex assay (data not shown). IL-8 secretion by ELISA was not significantly different, and IL-8 receptor I (C-X-C chemokine receptor type 1) was not detectible in fibroblasts by Western blot or quantitative polymerase chain reaction. IL-2, IL-6, granulocyte-macrophage colony-stimulating factor, interferon-γ, IL-10, IL-12, and IL-1β were assayed in VEDS and control samples but were below the standard curve limits according to an MSD multiplex assay (data not shown). Circulating biomarkers in VEDS were compared with a cohort of MFS patients (n=20). CRP and SAA were different between groups, with CRP significantly elevated ($P=0.046$) in VEDS but not MFS ($P=0.075$) and SAA significantly elevated in MFS ($P=0.037$) but not in VEDS ($P=0.074$; see Data Supplement Table I).

Because haploinsufficient patients with VEDS reportedly have a milder phenotype and later onset of complications,[9,10] all biomarkers (TGF-β1, TGF-β2, MCP-1, CRP, ICAM-1,

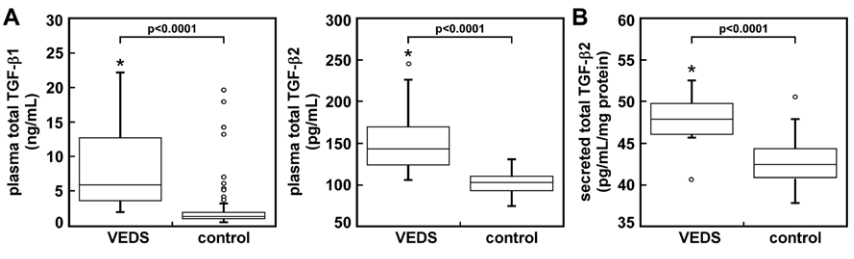

Figure 1. Circulating and secreted transforming growth factor (TGF)-β in vascular Ehlers–Danlos syndrome (VEDS) by ELISA. **A**, Box-and-whisker plots reveal elevated total TGF-β1 and -β2 in platelet-poor EDTA-plasma from VEDS subjects (n=35) vs healthy controls (n=74). **B**, Box-and-whisker plots reveal secreted total TGF-β2, but not TGF-β1 or -β3, from VEDS subject fibroblasts (n=17) is elevated vs healthy controls (n=17) ex vivo. Secretion data are normalized to protein concentration.

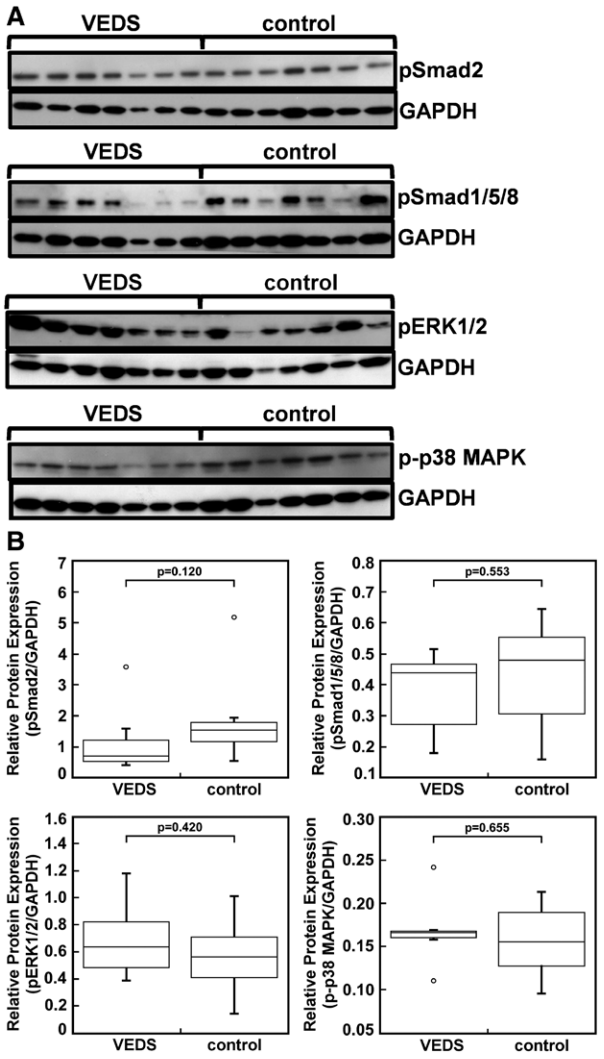

Figure 2. Western blot analysis of transforming growth factor (TGF)-β biomarkers in dermal fibroblasts. **A**, Whole cell lysate from vascular Ehlers–Danlos syndrome (VEDS) subject (n=17) and control fibroblasts (n=17) probed for pSmad2 and pSmad1/5/8, treated with TGF-β1 or BMP-4, respectively, or untreated pERK1/2 and p-p38 mitogen-activated protein kinase (MAPK) revealed no significant differences. **B**, Box-and-whisker plots showing the Western blot quantification are shown. Data are normalized to the loading control; however, the same results are seen when normalized to total protein ($P \leq 0.05$ considered significant). Representative blots are shown; however, quantification graphs include all samples above.

VCAM-1, IL-8, and leptin) were correlated to the individual mutation type and patient clinical history (ie, probands versus ITFH). ICAM-1 and VCAM-1 were significantly higher in the ES group versus the gly group (P=0.05 and P=0.006, respectively) and the null group (P=0.02 and P=0.01, respectively; Figure 5A). CRP was significantly higher in patients identified as probands versus ITFH (P=0.01; Figure 5B). ICAM-1 and VCAM-1 also showed a similar trend to CRP with increases in the probands versus the ITFH group, but results were not statistically significant (P>0.05). None of the other biomarkers studied showed a significant difference between groups, indicating that, with the exception of CRP, disease severity or complications were not factors.

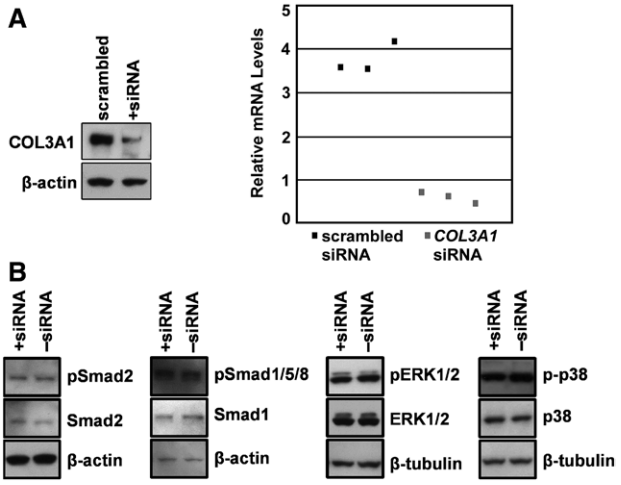

Figure 3. *COL3A1* gene silencing by allele-specific small interfering RNA (siRNA). **A**, Knockdown of the dominant negative mutant allele in *COL3A1* in fibroblasts of a patient with vascular Ehlers–Danlos syndrome (VEDS) is shown by quantitative polymerase chain reaction (qPCR) and Western blot. mRNA and protein expression are reduced after adding *COL3A1* allele-specific siRNA vs a nonspecific siRNA. qPCR data are normalized to *18S* mRNA, and protein data are normalized to β-actin. **B**, Western blot analysis of dermal fibroblasts from the VEDs patient treated with *COL3A1* allele-specific siRNA vs no siRNA shows no change in transforming growth factor-β pathway biomarkers, consistent with Figure 1. Data are normalized to the loading control; however, the same results are seen when normalized to total protein ($P \leq 0.05$ considered significant).

To determine whether medications taken by the patients with VEDS at the time of sample collection affected the circulating and secreted biomarkers, their concentrations were analyzed as above. Specifically, only medications with known cardiovascular effects were considered, including β-blockers (n=16), statins (n=7), and aspirin (n=6), whereas angiotensin receptor blockers (n=4), angiotensin-converting enzyme inhibitors (n=3), and calcium channel blockers (n=3) were not included because of insufficient sample size. Eighteen patients were on none of these medications. For the remaining individual groups, the levels of TGF-β1, TGF-β2, MCP-1, CRP, ICAM-1, VCAM-1, IL-8, and leptin remained significantly higher (or lower for IL-8) in the VEDS/β-blocker group versus controls ($P \leq 0.05$, same trend as entire VEDS cohort regardless of drug intervention, in Figures 1 and 4). For patients with VEDS on statins, only plasma TGF-β2 and IL-8 remained significantly higher and lower, respectively, than controls ($P \leq 0.05$). For patients with VEDS using aspirin, plasma TGF-β2, MCP-1, and IL-8 remained significantly higher and lower (IL-8), respectively, than controls ($P \leq 0.05$). Patients who had a previous event taking the above medications had significantly elevated IL-8 in circulation (P=0.007) versus patients without a previous event taking the above medications.

VEDS Body Composition Analysis

Dual-energy x-ray absorptiometry scans that include body composition data[28] were available in a subset of patients with VEDS (n=20; 13 of 20 probands; 7 of 20 ITFH; 9 gly; 4 ES; 4 null; 3 other mutation) who were found to have an altered

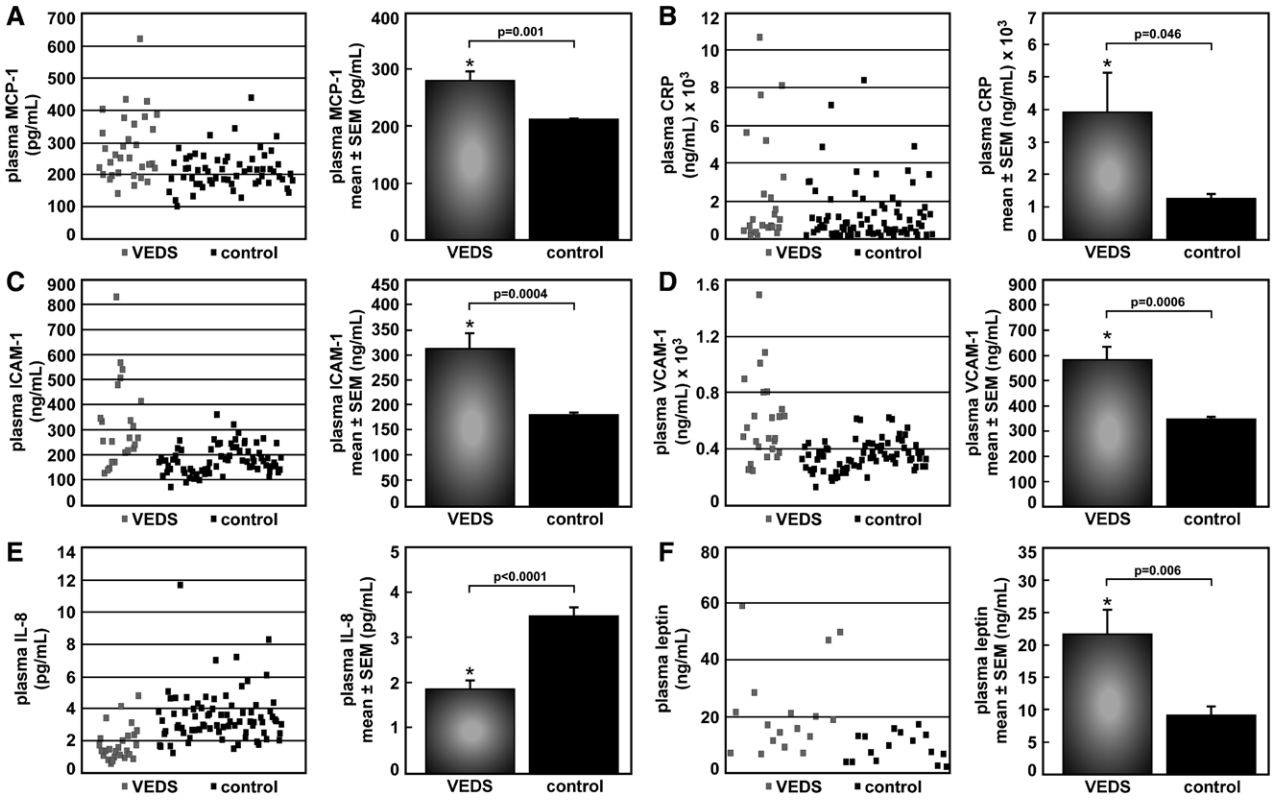

Figure 4. Circulating inflammatory biomarkers and adipokines in vascular Ehlers–Danlos syndrome (VEDS). **A**–**D** show evidence of systemic inflammation through elevated inflammatory markers monocyte chemotactic protein-1 (MCP-1), C-reactive protein (CRP), intercellular adhesion molecule-1 (ICAM-1), and vascular cell adhesion molecule-1 (VCAM-1) in platelet-poor EDTA-plasma from VEDS subjects (n=35) vs healthy controls (n=74). Samples were assayed using an immuno-multiplex system. **E**, Reduced interleukin-8 (IL-8) is seen in platelet-poor EDTA-plasma from VEDS subjects vs healthy controls. **F**, Significantly increased leptin in platelet-poor EDTA-plasma by ELISA from VEDS subjects vs healthy controls is seen.

body fat distribution versus age-, sex-, and body mass index–matched controls (n=17; nominal values in Data Supplement Table II). The body mass index and total body fat mass were not significantly different (P>0.05); however, truncal fat was significantly increased in VEDS versus controls (P<0.001). The leg fat/total fat ratio was significantly decreased in VEDS (P<0.001), whereas the trunk fat/total fat ratio was significantly increased in VEDS (P<0.001) versus controls (Figure 6). We found a weak, positive correlation between TGF-β1 and trunk fat (r=0.16) in patients who had an event and a weak, negative correlation between TGF-β1 and trunk fat (r=–0.22) in patients who did not suffer an event.

Mean Platelet Volume

The MPV, a platelet turnover indicator, was significantly elevated in VEDS versus healthy controls (P=0.0007), although there were no significant differences in the absolute platelet counts (P>0.05; Figure 7). MPV remained significantly

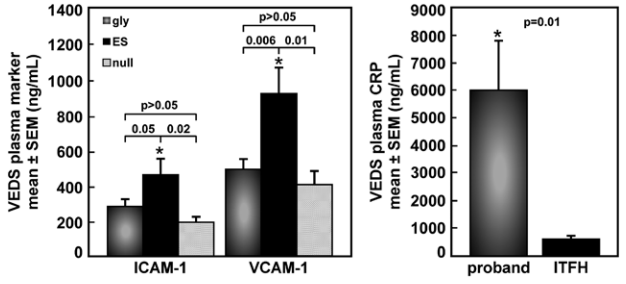

Figure 5. Clinical analysis of biomarkers in vascular Ehlers–Danlos syndrome (VEDS). **A**, Patients with VEDS identified with exon skipping mutations (n=6) have elevated intercellular adhesion molecule-1 (ICAM-1) and vascular cell adhesion molecule-1 (VCAM-1) vs patients with glycine substitutions (n=11) or null mutations (n=6) resulting in *COL3A1* haploinsufficiency. **B**, Patients with VEDS identified as probands (n=16) have increased C-reactive protein (CRP) vs patients identified through family history (ITFH; n=10).

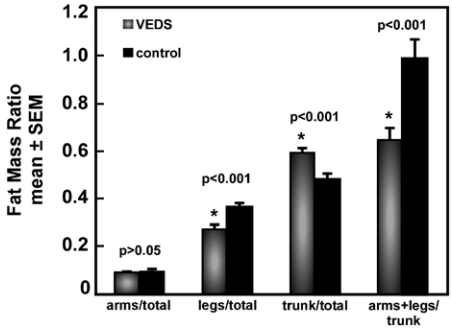

Figure 6. Body composition analysis in vascular Ehlers–Danlos syndrome (VEDS) patients. Body fat distribution by dual energy X-ray absorptiometry scan in patients with VEDS (n=20) vs healthy controls (n=17) is shown. Increased truncal fat but decreased limb fat is seen; however, the total fat mass between groups is the same.

elevated in the proband (P=0.02) and ITFH (P=0.01) subgroups versus controls.

Discussion

TGF-β signaling pathway abnormalities have been implicated in several connective tissue dysplasias with some overlapping but distinct phenotypes. In VEDS, the aneurysms and dissections usually occur in the medium-sized arteries rather than the aortic root,[1] and there is no evidence of long-bone overgrowth seen in MFS, where mutations in *FBN1* lead to increased circulating TGF-β1[29] and intracellular TGF-β1 signaling.[12,13] In Loeys–Dietz syndrome, mutations in *TGFBR1*, *TGFBR2*, *TGFB2*, and *SMAD3* may result in vascular, obstetric, and skin abnormalities similar to VEDS.[14–16,30,31] However, features such as bifid uvula, hypertelorism, and craniosynostosis are not found in VEDS. TGF-β2 deficiency is known to cause developmental defects involving the heart, lung, limb, spinal column, and craniofacial systems in animal models and inactivating mutations in *TGFB2* lead to familial thoracic aortic aneurysm with paradoxically elevated TGF-β2 in tissue.[15,32,33]

We found that proinflammatory markers TGF-β1, TGF-β2, MCP-1, CRP, ICAM-1, and VCAM-1 were elevated, and IL-8 was decreased in circulation in VEDS subjects versus controls. No differences were found between probands and patients with VEDS who were identified through relatives and who had no complications themselves, indicating that elevated TGF-β1 and -β2 may correlate to having the disease but not necessarily to disease severity or activity. MPV, a platelet turnover indicator, was significantly increased in VEDS. TGF-β1 is known to be abundant in platelets,[34] which was the rationale for performing measurements in platelet-free plasma. Ongoing microvascular damage, even in younger patients without complications, may lead to increased platelet turnover, degranulation, and subsequent TGF-β1 release into circulation as recently described in a mouse model of cardiac pressure overload.[35] Interestingly, we found that CRP was not significantly elevated in MFS, suggesting a different biomarker profile from VEDS.

Cardiovascular medication use in patients with VEDS modulated TGF-β1, MCP-1, CRP, ICAM-1, VCAM-1, and leptin levels. ICAM-1 and VCAM-1 correlated with VEDS severity. Although the exact role of these proteins is unclear, both markers are increased in atherosclerotic lesions in human coronary arteries,[36] indicating a role in injury response. MCP-1 mediates vascular inflammatory cell adhesion and contributes to neointimal hyperplasia in arterial injury.[37] Elevated CRP is seen in acquired autoimmune disorders and concentrations correlate with inflammation extent and severity.[38] Increased CRP has been found in patients with osteoarthritis and progressive joint damage,[39] as well as coronary disease.[40] We postulate that there is underlying chronic vascular damage in VEDS that alters the vascular environment and may lead to a state of systemic inflammation (MCP-1 and CRP elevation), which may contribute to adverse clinical outcomes. Although CRP levels did not correlate with mutation type, the significant increase in probands versus patients with ITFH suggests that CRP may be a disease activity indicator; therefore, monitoring CRP levels in patients with VEDS should be considered. If elevated, we would recommend shorter arterial surveillance intervals and a low threshold for working up new symptoms/signs with imaging studies. We would also recommend aggressively addressing all cardiovascular risk factors that increase aneurismal event risk (eg, elevated blood pressure, abnormal lipids, smoking) to improve outcomes.

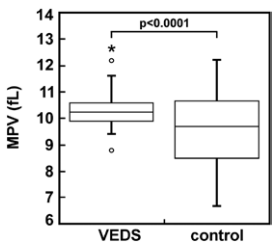

Figure 7. Mean platelet volume (MPV). The MPV was measured in plasma of patients with vascular Ehlers–Danlos syndrome (VEDS) (n=35) vs healthy controls (n=74). Significant platelet turnover is seen by increased MPV in patients with VEDS.

Secreted TGF-β2, but not TGF-β1, from VEDS fibroblasts was elevated versus controls. TGF-β2 is much less abundant than TGF-β1 in circulation and in tissues,[34] and the finding of excess circulating levels and increased secretion ex vivo in extracellular matrix–producing cells allows the possibility for a role of TGF-β2 in VEDS pathogenesis, different from that of TGF-β1. Interestingly, Western blot analysis of downstream TGF-β biomarkers and mRNA analysis of TGF-β pathway genes in fibroblasts did not reveal any differences between VEDS subjects and controls. Furthermore, treating fibroblasts of a patient with VEDS with allele-specific siRNA, which converted the gly-type mutation to a null-type, showed that suppressing the structurally abnormal type III collagen did not alter TGF-β signaling downstream of the receptors. Dermal fibroblasts historically have been used to study VEDS because the disease has a strong skin phenotype, mimicking the fragility found in vascular tissues. Therefore, we found it noteworthy that the underlying genetic defect did not impair intracellular TGF-β signaling in this setting when the expectation would be that it should. Although intracellular changes were not found in fibroblasts, it is possible that studying other cell types (eg, vascular smooth muscle) may demonstrate an effect. The lack of available direct tissue for study precluded the investigation of TGF-β1 and TGF-β2 or downstream targets in VEDS arteries. However, this could be undertaken in the future, especially through development of an animal model recapitulating the vascular complications of VEDS, specifically, medium-sized artery aneurysms and dissections. An appropriate animal model does not currently exist.

Interestingly, TGF-β2 and IL-8 were the only analytes in plasma unaffected by the drug treatments. IL-8 was decreased in VEDS versus controls. IL-8 plays an important role in angiogenesis,[41,42] and TGF-β1 inhibits IL-8 secretion during active inflammation in the vascular endothelium, consistent with our findings.[43] A potential role for reduced IL-8 in VEDS and related aneurismal disorders is intriguing and warrants further study. Although the absence of modulation by cardiovascular medications suggests that TGF-β2 and IL-8 may have intrinsic correlations to the disease, caution needs to be exercised in interpreting these data because the study design does not allow for a rigorous analysis of drug effects.

Leptin levels were significantly increased (but adiponectin unchanged) in VEDS plasma. Body composition analysis showed that patients with VEDS have increased truncal fat mass versus controls. Excess TGF-β1 release by human adipose tissue in obesity has been described but not TGF-β2[44]; however, our study subjects are not obese. In a recent study of an Italian VEDS cohort, a similar truncal fat distribution was seen versus controls, suggesting that this is not a diet-dependent effect.[45] In the general population, regional adiposity is known to be associated with arterial stiffness through the influence of leptin.[46] Abdominal adiposity markers have a graded and significant association with risk of stroke/transient ischemic attack.[47] In VEDS, the vascular condition is inborn and predates the fat deposition pattern. Although the sample size was small, we found a weak correlation between TGF-β1 and trunk fat in patients who had an event. Therefore, it is possible that vascular inflammation is leading to the abnormal truncal fat accumulation rather than the reverse. However, a prospective study would be needed to confirm this hypothesis.

There are several limitations to this study. We used available dermal fibroblasts because an appropriate mouse model and arterial tissues were not available. Although we expect to see a phenotype in VEDS dermal fibroblasts, we acknowledge that other types of extracellular matrix–producing cells, such as vascular smooth muscle, may yield different results. A VEDS mouse model would permit a more thorough TGF-β pathway examination at the tissue level, which again was not feasible with the study's limited human samples. Samples sizes were relatively limited in this study; therefore, analyses in a larger cohort are warranted to confirm the results. We were unable to perform uniform and exhaustive vascular imaging in all subjects to detect asymptomatic aneurysms or dissections; therefore, a rigorous correlation of vascular lesions with study biomarkers could not be done. Finally, fresh plasma samples, required for more accurate platelet turnover measurements compared with MPV values, were no longer available when we considered the possibility of excess platelet turnover as a source of elevated TGF-β1.

In summary, we present evidence for changes in biomarker profiles in VEDS that include TGF-β1, TGF-β2, MCP-1, CRP, ICAM-1, VCAM-1, IL-8, and leptin. The absence of correlations with mutation type and disease severity for all but 1 (CRP) of the biomarkers studied suggests ongoing microvascular damage in patients with VEDS even in the absence of an event. TGF-β2 and IL-8 are altered and not affected by current drug treatment and could underlie disease specificity, unlike TGF-β1. The evidence for excess TGF-β2 secretion from VEDS fibroblasts independent of the organismal milieu suggests a probable role. Regional truncal adiposity and elevated leptin in VEDS point to the role of microvascular damage in adipocyte deposition and dysfunction. Finally, these data represent the first evidence for a preinflammatory state in VEDS and, after validation in affected tissues, open the door to treatment strategies by targeting specific cytokine pathways.

Acknowledgments

We thank Dr Harry Dietz for study design contributions, study participants, the National Institute on Aging clinical unit and core laboratory for clinical support and sample processing, and Baltimore Longitudinal Study of Aging investigators for data use.

Sources of Funding

This research was supported, in part, by the Intramural Research Program of the National Institutes of Health, National Institute on Aging. Grants 1U54RR023561-01A1 and 5RC1HL100021-02 were used for plasma biomarker studies at Johns Hopkins.

Disclosures

None.

References

1. Pepin M, Schwarze U, Superti-Furga A, Byers PH. Clinical and genetic features of Ehlers-Danlos syndrome type IV, the vascular type. *N Engl J Med*. 2000;342:673–680.
2. Pope FM, Martin GR, Lichtenstein JR, Penttinen R, Gerson B, Rowe DW, et al. Patients with Ehlers-Danlos syndrome type IV lack type III collagen. *Proc Natl Acad Sci U S A*. 1975;72:1314–1316.
3. Tsipouras P, Byers PH, Schwartz RC, Chu ML, Weil D, Pepe G, et al. Ehlers-Danlos syndrome type IV: cosegregation of the phenotype to a COL3A1 allele of type III procollagen. *Hum Genet.* 1986;74:41–46.
4. Stolle CA, Pyeritz RE, Myers JC, Prockop DJ. Synthesis of an altered type III procollagen in a patient with type IV Ehlers-Danlos syndrome: a structural change in the alpha 1(III) chain which makes the protein more susceptible to proteinases. *J Biol Chem*. 1985;260:1937–1944.
5. Ong KT, Perdu J, De Backer J, Bozec E, Collignon P, Emmerich J, et al. Effect of celiprolol on prevention of cardiovascular events in vascular Ehlers-Danlos syndrome: a prospective randomised, open, blinded-endpoints trial. *Lancet*. 2010;376:1476–1484.
6. Tae HJ, Marshall S, Zhang J, Wang M, Briest W, Talan MI. Chronic treatment with a broad-spectrum metalloproteinase inhibitor, doxycycline, prevents the development of spontaneous aortic lesions in a mouse model of vascular Ehlers-Danlos syndrome. *J Pharmacol Exp Ther*. 2012;343:246–251.
7. Schwarze U, Goldstein JA, Byers PH. Splicing defects in the COL3A1 gene: marked preference for 5' (donor) spice-site mutations in patients with exon-skipping mutations and Ehlers-Danlos syndrome type IV. *Am J Hum Genet*. 1997;61:1276–1286.
8. Smith LT, Schwarze U, Goldstein J, Byers PH. Mutations in the COL3A1 gene result in the Ehlers-Danlos syndrome type IV and alterations in the size and distribution of the major collagen fibrils of the dermis. *J Invest Dermatol*. 1997;108:241–247.
9. Leistritz DF, Pepin MG, Schwarze U, Byers PH. COL3A1 haploinsufficiency results in a variety of Ehlers-Danlos syndrome type IV with delayed onset of complications and longer life expectancy. *Genet Med*. 2011;13:717–722.
10. Schwarze U, Schievink WI, Petty E, Jaff MR, Babovic-Vuksanovic D, Cherry KJ, et al. Haploinsufficiency for one COL3A1 allele of type III procollagen results in a phenotype similar to the vascular form of Ehlers-Danlos syndrome, Ehlers-Danlos syndrome type IV. *Am J Hum Genet*. 2001;69:989–1001.
11. Kim KL, Yang JH, Song SH, Kim JY, Jang SY, Kim JM, et al. Positive correlation between the dysregulation of transforming growth factor-β1 and aneurysmal pathological changes in patients with Marfan syndrome. *Circ J*. 2013;77:952–958.
12. Habashi JP, Judge DP, Holm TM, Cohn RD, Loeys BL, Cooper TK, et al. Losartan, an AT1 antagonist, prevents aortic aneurysm in a mouse model of Marfan syndrome. *Science*. 2006;312:117–121.
13. Neptune ER, Frischmeyer PA, Arking DE, Myers L, Bunton TE, Gayraud B, et al. Dysregulation of TGF-beta activation contributes to pathogenesis in Marfan syndrome. *Nat Genet.* 2003;33:407–411.
14. Drera B, Tadini G, Barlati S, Colombi M. Identification of a novel TGFBR1 mutation in a Loeys-Dietz syndrome type II patient with vascular Ehlers-Danlos syndrome phenotype. *Clin Genet*. 2008;73:290–293.
15. Lindsay ME, Schepers D, Bolar NA, Doyle JJ, Gallo E, Fert-Bober J, et al. Loss-of-function mutations in TGFB2 cause a syndromic presentation of thoracic aortic aneurysm. *Nat Genet.* 2012;44:922–927.
16. van de Laar IM, Oldenburg RA, Pals G, Roos-Hesselink JW, de Graaf BM, Verhagen JM, et al. Mutations in smad3 cause a syndromic form of aortic aneurysms and dissections with early-onset osteoarthritis. *Nat Genet.* 2011;43:121–126.
17. Cho HR, Hong SB, Kim YI, Lee JW, Kim NI. Differential expression of TGF-beta isoforms during differentiation of HaCaT human keratinocyte cells: implication for the separate role in epidermal differentiation. *J Korean Med Sci*. 2004;19:853–858.

18. Mortani Barbosa EJ Jr, Pyeritz RE, Litt H, Desjardins B. Vascular Ehlers-Danlos syndrome presenting as rapidly progressive multiple arterial aneurysms and dissections. *Am J Med Genet A*. 2011;155A:3090–3094.
19. St. Hilaire C, Ziegler SG, Markello TC, Brusco A, Groden C, Gill F, et al. NT5E mutations and arterial calcifications. *N Engl J Med*. 2011;364:432–442.
20. Doyle AJ, Doyle JJ, Bessling SL, Maragh S, Lindsay ME, Schepers D, et al. Mutations in the TGF-β repressor SKI cause Shprintzen-Goldberg syndrome with aortic aneurysm. *Nat Genet.* 2012;44:1249–1254.
21. Aoyama T, Francke U, Gasner C, Furthmayr H. Fibrillin abnormalities and prognosis in Marfan syndrome and related disorders. *Am J Med Genet*. 1995;58:169–176.
22. Müller GA, Hansen U, Xu Z, Griswold B, Talan MI, McDonnell NB, et al. Allele-specific siRNA knockdown as a personalized treatment strategy for vascular Ehlers-Danlos syndrome in human fibroblasts. *FASEB J*. 2012;26:668–677.
23. Kontusaari S, Tromp G, Kuivaniemi H, Romanic AM, Prockop DJ. A mutation in the gene for type III procollagen (COL3A1) in a family with aortic aneurysms. *J Clin Invest*. 1990;86:1465–1473.
24. Johnson PH, Richards AJ, Lloyd JC, Pope FM, Hopkinson DA. Efficient strategy for the detection of mutations in acrogeric Ehlers-Danlos syndrome type IV. *Hum Mutat.* 1995;6:336–342.
25. Kontusaari S, Tromp G, Kuivaniemi H, Ladda RL, Prockop DJ. Inheritance of an RNA splicing mutation (G+ 1 IVS20) in the type III procollagen gene (COL3A1) in a family having aortic aneurysms and easy bruisability: phenotypic overlap between familial arterial aneurysms and Ehlers-Danlos syndrome type IV. *Am J Hum Genet*. 1990;47:112–120.
26. Persikov AV, Pillitteri RJ, Amin P, Schwarze U, Byers PH, Brodsky B. Stability related bias in residues replacing glycines within the collagen triple helix (Gly-Xaa-Yaa) in inherited connective tissue disorders. *Hum Mutat.* 2004;24:330–337.
27. Kuivaniemi H, Kontusaari S, Tromp G, Zhao MJ, Sabol C, Prockop DJ. Identical G+1 to A mutations in three different introns of the type III procollagen gene (COL3A1) produce different patterns of RNA splicing in three variants of Ehlers-Danlos syndrome: IV: an explanation for exon skipping some mutations and not others. *J Biol Chem*. 1990;265:12067–12074.
28. Andreoli A, Scalzo G, Masala S, Tarantino U, Guglielmi G. Body composition assessment by dual-energy X-ray absorptiometry (DXA). *Radiol Med*. 2009;114:286–300.
29. Matt P, Schoenhoff F, Habashi J, Holm T, Van Erp C, Loch D, et al; GenTAC Consortium. Circulating transforming growth factor-beta in Marfan syndrome. *Circulation*. 2009;120:526–532.
30. Loeys BL, Chen J, Neptune ER, Judge DP, Podowski M, Holm T, et al. A syndrome of altered cardiovascular, craniofacial, neurocognitive and skeletal development caused by mutations in TGFBR1 or TGFBR2. *Nat Genet.* 2005;37:275–281.
31. Loeys BL, Schwarze U, Holm T, Callewaert BL, Thomas GH, Pannu H, et al. Aneurysm syndromes caused by mutations in the TGF-beta receptor. *N Engl J Med*. 2006;355:788–798.
32. Boileau C, Guo DC, Hanna N, Regalado ES, Detaint D, Gong L, et al; National Heart, Lung, and Blood Institute (NHLBI) Go Exome Sequencing Project. TGFB2 mutations cause familial thoracic aortic aneurysms and dissections associated with mild systemic features of Marfan syndrome. *Nat Genet.* 2012;44:916–921.
33. Sanford LP, Ormsby I, Gittenberger-de Groot AC, Sariola H, Friedman R, Boivin GP, et al. TGFbeta2 knockout mice have multiple developmental defects that are non-overlapping with other TGFbeta knockout phenotypes. *Development*. 1997;124:2659–2670.
34. Derynck R, Jarrett JA, Chen EY, Eaton DH, Bell JR, Assoian RK, et al. Human transforming growth factor-beta complementary DNA sequence and expression in normal and transformed cells. *Nature*. 1985;316:701–705.
35. Meyer A, Wang W, Qu J, Croft L, Degen JL, Coller BS, et al. Platelet TGF-β1 contributions to plasma TGF-β1, cardiac fibrosis, and systolic dysfunction in a mouse model of pressure overload. *Blood*. 2012;119:1064–1074.
36. Davies MJ, Gordon JL, Gearing AJ, Pigott R, Woolf N, Katz D, et al. The expression of the adhesion molecules ICAM-1, VCAM-1, PECAM, and E-selectin in human atherosclerosis. *J Pathol.* 1993;171:223–229.
37. Ling S, Nheu L, Komesaroff PA. Cell adhesion molecules as pharmaceutical target in atherosclerosis. *Mini Rev Med Chem*. 2012;12:175–183.
38. Gabay C, Kushner I. Acute-phase proteins and other systemic responses to inflammation. *N Engl J Med*. 1999;340:448–454.
39. Spector TD, Hart DJ, Nandra D, Doyle DV, Mackillop N, Gallimore JR, et al. Low-level increases in serum C-reactive protein are present in early osteoarthritis of the knee and predict progressive disease. *Arthritis Rheum*. 1997;40:723–727.
40. Ridker PM, Cushman M, Stampfer MJ, Tracy RP, Hennekens CH. Inflammation, aspirin, and the risk of cardiovascular disease in apparently healthy men. *N Engl J Med*. 1997;336:973–979.
41. Koch AE, Polverini PJ, Kunkel SL, Harlow LA, DiPietro LA, Elner VM, et al. Interleukin-8 as a macrophage-derived mediator of angiogenesis. *Science*. 1992;258:1798–1801.
42. Li A, Dubey S, Varney ML, Dave BJ, Singh RK. IL-8 directly enhanced endothelial cell survival, proliferation, and matrix metalloproteinases production and regulated angiogenesis. *J Immunol.* 2003;170:3369–3376.
43. Smith WB, Noack L, Khew-Goodall Y, Isenmann S, Vadas MA, Gamble JR. Transforming growth factor-beta 1 inhibits the production of IL-8 and the transmigration of neutrophils through activated endothelium. *J Immunol.* 1996;157:360–368.
44. Fain JN, Tichansky DS, Madan AK. Transforming growth factor beta1 release by human adipose tissue is enhanced in obesity. *Metabolism*. 2005;54:1546–1551.
45. Ritelli M, Drera B, Zoppi N, Tadini G, Venturini M, Wischmeijer A, et al. Abstract: diagnosis of vascular Ehlers-Danlos syndrome in Italy: clinical findings and novel col3a1 mutations. *First International Symposium on the Ehlers-Danlos Syndrome*. Ghent, Belgium. 2012:16.
46. Windham BG, Griswold ME, Farasat SM, Ling SM, Carlson O, Egan JM, et al. Influence of leptin, adiponectin, and resistin on the association between abdominal adiposity and arterial stiffness. *Am J Hypertens*. 2010;23:501–507.
47. Winter Y, Rohrmann S, Linseisen J, Lanczik O, Ringleb PA, Hebebrand J, et al. Contribution of obesity and abdominal fat mass to risk of stroke and transient ischemic attacks. *Stroke*. 2008;39:3145–3151.

CLINICAL PERSPECTIVE

We explored the role of transforming growth factor-β pathway and other inflammatory biomarkers in plasma and dermal fibroblasts from patients with vascular Ehlers–Danlos syndrome (VEDS), which is caused by mutations in the *COL3A1* gene. Analyses were done in terms of clinical disease severity, genotype–phenotype correlations, and body composition and fat deposition alterations. VEDS subjects were found to have elevated transforming growth factor-β1, transforming growth factor-β2, monocyte chemotactic protein-1, C-reactive protein, intercellular adhesion molecule-1, and vascular cell adhesion molecule-1 in circulation compared with controls. Adipocyte dysfunction in VEDS was demonstrated through elevated leptin and decreased interleukin-8 in circulation. Dermal fibroblasts from VEDS subjects secreted greater amounts of transforming growth factor-β2 compared with controls. Patients with *COL3A1* exon skipping mutations had higher plasma intercellular adhesion molecule-1 and vascular cell adhesion molecule-1, and VEDS probands had abnormally high plasma C-reactive protein compared with affected patients identified through family members before any disease manifestations. Patients with VEDS had higher mean platelet volumes, suggesting increased platelet turnover because of ongoing vascular damage, as well as increased regional truncal adiposity. C-reactive protein is linked to disease state and may be a disease activity marker. These findings suggest that VEDS is a systemic disease with a major inflammatory component, and the above biomarkers should be considered when assessing patients with VEDS in the clinic.

Supplemental Material

Supplemental Methods

Genetic Mutation Analysis

All VEDS subjects included in this study have a pathogenic mutation confirmed in *COL3A1*. The coding regions and flanking sequences of the *COL3A1* gene were amplified and sequenced. Primers were designed by Primer3 (http://frodo.wi.mit.edu/primer3/) and are available upon request. Mutations were identified by alignment with the reference sequence (ENSG00000168542). Some patients had mutation detection for *COL3A1* or biochemical analysis of procollagen III performed by a CLIA certified laboratory prior to enrollment, which was confirmed in our laboratory. One patient (Patient 41) with multiple dissections had a *de novo* Pro1440Ser mutation. The parents were negative for the mutation, as verified by a CLIA-certified lab, and were clinically unaffected. Additionally, *in silico* analysis suggested pathogenicity (see main text under Results, Genetic Analysis).

Fibroblast Cell Culture

We use established protocols to derive dermal fibroblast primary cell lines from 4-mm punch skin biopsy samples obtained from the forearm of study participants who consented to a biopsy.[1] Fibroblast cultures below passage ten from VEDS subjects and age-, sex-, and passage-matched healthy controls were cultured to confluence in high glucose Dulbecco's modified Eagle's medium, 10.0% fetal bovine serum, penicillin, and streptomycin (Invitrogen, Carlsbad, CA, USA) at 37°C in 5.0% CO_2. For Western blot experiments, untreated cells (for pERK1/2 and p-p38) were grown to confluence before lysis. Treated cells were grown to ~80% confluence

then serum starved for 18 hours. Cells were then treated for 1 hour with either 10 ng/mL TGF-β1 (for pSmad2) or 50 ng/mL BMP-4 (for pSmad1/5/8) (R&D Systems, Minneapolis, MN, USA).

ELISA Assays

For secretion experiments, background TGF-β found in bovine serum was eliminated by a series of washes with serum free medium and then incubation with serum free medium for 24 hours. Total TGF-β1, -β2, and -β3 concentrations in secreted medium from human skin fibroblast cell lines that provided adequate *in vitro* cell growth (n = 17 VEDS, 17 controls) and total TGF-β2 in platelet-poor EDTA-plasma (n = 35 VEDS, 74 controls) were measured by enzyme-linked immunosorbent assay with the human TGF-β1 and TGF-β2 Quantikine ELISA kits (R&D Systems, Minneapolis, MN) and the human TGF-β3 DuoSet ELISA kit (R&D Systems). Samples were acid-activated according to the manufacturer's instructions. Human leptin in platelet-poor EDTA-plasma was measured using the Human Leptin ELISA kit (Millipore) according to the manufacturer's instructions. Total TGF-β1, MCP-1, CRP, ICAM-1, VCAM-1, IL-8, and adiponectin in human plasma (n = 35 VEDS, 74 controls) were measured using a ruthenium-based commercially available electrochemiluminescence platform according to the manufacturer's instructions (Meso Scale Discovery, Gaithersburg, MD, USA). Samples used for TGF-β1 were acid-activated prior to assaying. All samples were assayed in duplicate. The percent coefficient of variance was below 20% and above the lower level of quantification for each analyte. Secretion data were normalized to protein concentration.

Western Blot Analysis

Fibroblasts were lysed with RIPA buffer (Pierce, Rockford, IL, USA) containing protease and phosphatase inhibitors (Cocktail Sets I, II, and III, Calbiochem, Gibbstown, NJ, USA) (n = 17 VEDs,

17 controls). Thirty µg protein (as determined by a BCA protein assay of whole cell protein extracts and using BSA as a standard, Pierce) was loaded onto a 4-12% Novex Tris-Glycine precast gel (Invitrogen). Proteins were then electrotransferred onto a PVDF membrane using Invitrogen's iBlot dry blotting system and immunoblotting was done using the appropriate human antibodies. Specifically, rabbit polyclonal anti-phospho-Smad1/5/8 (1:500, Cell Signaling Technology, Danvers, MA, USA), anti-Smad1 (1:500, Cell Signaling Technology), anti-phospho-Smad2 (1:500, Millipore, Billerica, MA, USA), anti-phospho-Erk1/2 (1:1000, Cell Signaling Technology), anti-p38 MAPK (1:500, Cell Signaling Technology), anti-COL3A1 (1:200, Santa Cruz Biotechnology, Inc, Santa Cruz, CA, USA), anti-β-tubulin (1:2,000, Cell Signaling Technology) or rabbit monoclonal anti-Smad2 (1:500, Cell Signaling Technology), anti-Erk1/2 (1:1000, Cell Signaling Technology), anti-phospho-p38 MAPK (1:500, Cell Signaling Technology), anti-GAPDH (1:2000, Cell Signaling Technology), anti-β-actin (1:1000, Cell Signaling Technology) were used overnight at 4°C, followed by 1 hour incubation with a secondary donkey anti-rabbit IgG ECL-HRP linked antibody (1:5000, GE Healthcare, Piscataway, NJ, USA). Immunoreactive products were visualized by chemiluminescence using the ECL Plus kit (GE Healthcare). Quantification of immunoblots was performed using ImageJ software (NIH, Bethesda, MD, USA) and was done within the linear range for each antibody.

RT^2 Profiler PCR Array System

RNA was extracted as described above. An RT^2 First Strand Kit (SABiosciences, Valencia, CA, USA) was used to synthesize cDNA using 1 µg RNA. Real-time PCR reactions and all recommended quality controls were run in 96-well Human TGF-β/BMP Signaling Pathway plates (SABiosciences) using SABiosciences RT^2 qPCR Master Mix according to the manufacturer's

directions. Data analysis was done using the $\Delta\Delta C_T$ method on the SABiosciences PCR Data Analysis Web Portal (http://www.SABiosciences.com/pcrarraydataanalysis.php).

Quantitative Real-Time PCR

An RNeasy Plus Mini kit (Qiagen, Valencia, CA, USA) was used to extract RNA according to the manufacturer's instructions. Synthesis of cDNA was done using 100 ng RNA and the qScript cDNA SuperMix (Quanta Biosciences, Gaithersburg, MD, USA). Gene expression was quantified using the SYBR green (Quanta Biosciences) method of real-time PCR and mRNA levels were compared to standard curves and normalized to *18S* mRNA. PCR reactions were performed in triplicate with QuantumRNA Universal 18S primers (Ambion, Grand Island, NY, USA) or 200 nM of each gene specific primer. The primers used for the human genes were designed to cross intron-exon junctions and are as follows: *ACVR2A* [forward (5'-CTGCTGCAAAGTTGGCGTTT-3') and reverse (5'-ACGGTTCAACACCAGTTTGAT-3')], *FOS* [forward (5'-CGGGCTTCAACGCAGACTA-3') and reverse (5'-GGTCCGTGCAGAAGTCCTG-3')], *ID1* [forward (5'-ACGAGCAGCAGGTAAACGTG-3') and reverse (5'-GAAGGTCCCTGATGTAGTCGAT-3')], *IL6* [forward (5'-AAATTCGGTACATCCTCGACGG-3') and reverse (5'- GGAAGGTTCAGGTTGTTTTCTGC-3')], *INHBB* [forward (5'-GTGAAGCGGCACATCTTGAG-3') and reverse (5'-GCGAAGCTGATGATTTCGGAAAC-3')], *STAT1* [forward (5'-ATGTCTCAGTGGTACGAACTTCA-3') and reverse (5'-TGTGCCAGGTACTGTCTGATT-3')], *TGFB2* [forward (5'- CTGCATCTGGTCACGGTCG-3') and reverse (5'- CCTCGGGCTCAGGATAGTCT-3')], and *TGFBR1* [forward (5'-ACGGCGTTACAGTGTTTCTG-3') and reverse (5'- GCACATACAAACGGCCTATCT-3')] (Integrated DNA Technologies, Coralville, IA, USA). Quantitative PCR was performed on an ABI Prism 7300 (Applied Biosystems, Carlsbad, CA, USA) sequence detection system using standard conditions.

Supplemental Results

Array and qPCR Analysis of TGF-β Pathway Genes in VEDS Dermal Fibroblasts

A human TGF-β/BMP signaling pathway array (SABiosciences) was used to screen for 84 genes of interest in VEDS. Each plate was designed to accept one cDNA sample at a time, therefore two plates were used, one VEDS patient and one control, to narrow down genes that might be up- or down-regulated greater than 2-fold in VEDS compared to a control. After a panel of genes was identified (*ACVR2A, FOS, ID1, IL6, INHBB, STAT1, TGFB2, TGFBR1*), these were tested in a larger cohort of 12 patients and 12 healthy controls using qPCR. It was found that a large amount of variation existed in each population for each gene, as seen in a Whisker plot, but no significant gene of interest could be identified, lending support to the hypothesis that the observed aberrant TGF-β signaling in circulation and secreted from fibroblasts was not due to an intrinsic genetic defect (**Supplemental Figure 1**).

Supplemental Figure Legends

Supplemental Figure 1 – qPCR expression analysis of TGF-β pathway genes in dermal fibroblasts. A TGF-β pathway gene array using a single VEDS patient and control narrowed down several candidate pathway markers that differed more than 2-fold between the two samples. However, qPCR analysis of these target genes using 12 patients and controls each revealed no significant differences in any TGF-β pathway genes tested. The Whisker plot and table shows the results and outliers that represent the range of normal human variation found in these genes.

Supplemental Tables

Supplemental Table 1. Circulating biomarker comparison between VEDS and MFS†.

Marker	VEDS (n = 35)		MFS (n = 20)		Control (n = 74)
	mean ± SEM	**P value**	**mean ± SEM**	**P value**	**mean ± SEM**
***CRP (ng/mL)**	3911 ± 1248	**0.046**	2700 ± 747	**0.075**	1264 ± 171
***SAA (ng/mL)**	5554 ± 2288	**0.074**	3142 ± 825	**0.037**	1281 ± 104
TNF-α (pg/mL)	4.99 ± 0.38	0.089	5.04 ± 0.30	0.069	4.33 ± 0.18
TGF-β1 (ng/mL)	8263 ± 1054	<0.0001	9171 ± 1360	0.0001	2470 ± 416
MCP-1 (pg/mL)	279 ± 18	0.001	270 ± 15	0.0004	211 ± 0.7
ICAM-1 (ng/mL)	313 ± 33	0.0004	265 ± 27	0.005	179 ± 6
VCAM-1 (ng/mL)	580 ± 58	0.0006	542 ± 40	0.0001	347 ± 12
IL-8 (pg/mL)	1.85 ± 0.21	<0.0001	1.98 ± 0.21	<0.0001	3.46 ± 0.18

P ≤ 0.05 considered significant; SEM – standard error of the mean. †MFS – Marfan syndrome

Supplemental Table 2. Patient Characteristics for Body Composition Analysis.

Patient No.	Sex	Age at Visit	Height (cm)	Weight (kg)	BMI
1	M	51	181	95	29.0
3	F	49	157	70	28.4
4	F	50	160	68	26.6
7	M	30	168	76	26.9
9	M	41	180	85	26.2
11	F	60	160	76	29.7
12	F	38	161	71	27.4
19	F	36	147	46	21.3
24	F	47	168	77	27.3
25	M	26	174	84	27.7
29	F	30	159	63	24.9
30	F	29	173	68	22.7
31	F	40	158	62	24.8
32	F	42	149	56	25.2
34	M	22	171	49	16.8
35	F	28	156	50	20.5
37	M	41	176	91	29.4
39	F	53	163	71	26.7
40	F	43	162	60	22.9

41	F	39	152	59	25.5
Control No.	**Sex**	**Age**	**Height (cm)**	**Weight (kg)**	**BMI**
1	M	39	177	92	29.4
2	F	53	162	55	21.0
3	F	50	164	57	21.2
4	F	43	177	66	21.1
5	F	38	167	59	21.2
6	F	60	160	67	26.2
7	F	28	165	74	27.2
8	F	42	165	63	23.1
9	F	42	163	58	21.8
10	F	44	166	70	25.4
11	F	55	167	69	24.7
12	F	26	180	76	23.5
13	M	43	186	80	23.1
14	M	30	189	88	24.6
15	F	47	164	72	26.8
16	M	27	198	75	19.1
17	F	35	164	60	22.3

Supplemental Figures

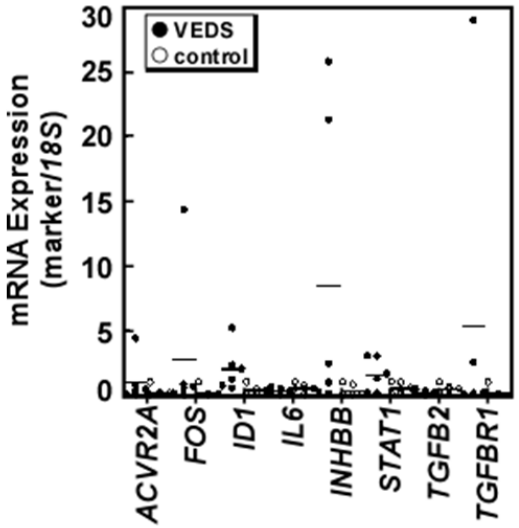

Gene	Relative mRNA Expression (mean ± SEM)		p-value
	VEDS	control	
ACVR2A	1.0 ± 0.7	2.7 ± 2.3	0.498
FOS	2.0 ± 0.7	0.33 ± 0.08	0.064
ID1	8.5 ± 4.8	1.6 ± 0.5	0.211
IL6	5.3 ± 4.8	0.22 ± 0.06	0.333
INHBB	0.76 ± 0.36	0.16 ± 0.04	0.157
STAT1	6.4 ± 3.4	2.2 ± 0.6	0.280
TGFB2	8.2 ± 5.1	0.59 ± 0.16	0.193
TGFBR1	0.49 ± 0.13	0.14 ± 0.02	0.040

Supplemental Figure 1

Supplemental References

1. Normand J, Karasek MA. A method for the isolation and serial propagation of keratinocytes, endothelial cells, and fibroblasts from a single punch biopsy of human skin. *In Vitro Cell Dev Biol Anim*. 1995;31:447-455.